

Synthesis, Reactivity, and Kinetics of Substitution in W_3PdSe_4 Cuboidal Clusters. A Reexamination of the Kinetics of Substitution of the Related W_3S_4 Cluster with Thiocyanate

Andrés G. Algarra,[†] Maxim N. Sokolov,^{‡,§} Javier González-Platas,^{||} María Jesús Fernández-Trujillo,[†] Manuel G. Basallote,^{*,†} and Rita Hernández-Molina^{*,†}

Departamento de Ciencia de los Materiales e Ingeniería Metalúrgica y Química Inorgánica, Facultad de Ciencias, Universidad de Cádiz, 11510 Puerto Real, Cádiz, Spain, A. V. Nikolaev Institute of Inorganic Chemistry, Pr. Laurentieva 3, 630090 Novosibirsk, Russian Federation, Novosibirsk State University, ul Pirogova 2, 630090 Novosibirsk, Russian Federation, Departamento de Física Fundamental II, Servicio de Difracción de Rayos X, Universidad de La Laguna, 38204 La Laguna, Tenerife, Spain, and Departamento de Química Inorgánica, Universidad de La Laguna, 38200 La Laguna, Tenerife, Islas Canarias, Spain

Received November 10, 2008

The reaction of $Pd(dba)_2$ ($dba = \text{dibenzylideneacetone}$) with $[W_3Se_4(H_2O)_9]^{4+}$ in 2 M HCl gives the cuboidal cluster $[W_3(PdCl)Se_4(H_2O)_9]^{3+}$, which undergoes edge-to-edge condensation and crystallizes from Hpts solutions as edge-linked double-cubane cluster $[(W_3PdSe_4(H_2O)_9)_2](pts)_8 \cdot 18H_2O$ ($pts^- = p\text{-toluenesulfonate}$). The substitution of Cl^- by different ligands, including phenylsulfinate $PhSO_2^-$, was explored. The phenylsulfinate complex was crystallized as a 2:1 adduct with cucurbit[6]uril ($C_{36}H_{36}N_{24}O_{12}$), $[W_3(Pd(PhSO_2)Se_4(H_2O)_{8.58}Cl_{0.42})_2(C_{36}H_{36}N_{24}O_{12})Cl_{5.16} \cdot 16.83H_2O$, and its structure was determined by X-ray diffraction. Solution studies indicate that the Pd atom is able to stabilize the pyramidal tautomer of hypophosphorous and phosphorous acid: $HP(OH)_2$ and $P(OH)_3$. Kinetic studies were carried out on the reactions with H_3PO_2 and thiocyanate, which were found to proceed in two and three kinetically resolvable steps, respectively. The kinetic results are discussed in terms of the mechanistic proposals put forward in the literature for related complexes. To gain insight into the details of the substitution kinetics in these kinds of clusters, the reaction of the related $[W_3S_4(H_2O)_9]^{4+}$ complex with NCS^- has been reexamined, and the results obtained provide for the first time information about the rates of substitution of the whole set of nine-coordinated water molecules.

Introduction

The chemistry of the heterometallic cuboidal clusters $M_3M'Q_4$ ($M = Mo, W$; $M' = \text{heterometal}$; $Q = S, Se$) has attracted much attention during the last 2 decades.^{1,2} When M' is Cu, Ni, or a noble metal (Pd, Ru), the resulting sulfido clusters are relevant to catalysis and their chemistry has been

reviewed.³ They display a rich chemistry at the heterometal site, including the ability to induce the isomerization^{4,5} of hydrophosphoryl molecules $H_2P(O)(OH)$, $HP(O)(OH)_2$, $PhP(O)(OH)(H)$, and $Ph_2P(O)(H)$ into their unstable hydroxo tautomers $HP(OH)_2$, $P(OH)_3$, $PhP(OH)_2$, and $Ph_2P(OH)$, which are stabilized by coordination to the heterometal atom. Hidai et al.⁶ were the first to succeed in the isolation of mixed-metal cubane-type sulfido clusters with the Mo_3PdS_4 core by preparing the cluster $[Mo_3(PdCl)S_4(H_2O)_9]^{3+}$ by a unique reaction of $[Mo_3S_4(H_2O)_9]^{4+}$ and Pd black in HCl. The studies on the Mo_3PdS_4 clusters have been prompted by their potential application as catalysts in a number of reactions such as stereo- and regioselective addition of alcohols or carboxylic acids to the alkynes and intramolecular cyclization of alkynoic acids, with a remarkably high efficiency.⁷

* To whom correspondence should be addressed. E-mail: manuel.basallote@uca.es (M.G.B.), rrhernan@ull.es (R.H.-M.).

[†] Universidad de Cádiz.

[‡] A. V. Nikolaev Institute of Inorganic Chemistry.

[§] Novosibirsk State University.

^{||} Departamento de Física Fundamental II, Servicio de Difracción de Rayos X, Universidad de La Laguna.

[†] Departamento de Química Inorgánica, Universidad de La Laguna.

(1) (a) Hernández-Molina, R.; Sokolov, M. N.; Sykes, A. G. *Acc. Chem. Res.* **2001**, *34*, 223. (b) Hernández-Molina, R.; Sykes, A. G. *J. Chem. Soc., Dalton Trans.* **1999**, 3137.

(2) Llusar, R.; Uriel, S. *Eur. J. Inorg. Chem.* **2003**, 1271.

The selenide $[\text{Mo}_3\text{Se}_4(\text{H}_2\text{O})_9]^{4+}$ reacts with Pd black in the same way.⁸ In contrast, no reaction was observed between Pd black and the tungsten clusters $[\text{W}_3\text{Q}_4(\text{H}_2\text{O})_9]^{4+}$ (Q = S, Se).⁸ The cuboidal cluster $[\text{W}_3(\text{PdCl})\text{S}_4(\text{H}_2\text{O})_9]^{3+}$ was obtained by the reaction of $[\text{W}_3\text{S}_4(\text{H}_2\text{O})_9]^{4+}$ with Pd⁰, generated in situ from H_3PO_2 and $[\text{PdCl}_4]^{2-}$.⁹ However, $[\text{PdCl}_4]^{2-}$ rapidly destroys $[\text{W}_3\text{Se}_4(\text{H}_2\text{O})_9]^{4+}$, and W_3PdSe_4 clusters could not be prepared in this way. In this paper, we report for the first time the preparation and reactivity studies of the cuboidal clusters with the W_3PdSe_4 core. Kinetic studies have been carried out on the reactions with H_3PO_2 (stabilization of $\text{HP}(\text{OH})_2$ at the Pd site) and NCS^- (substitution of coordinated water molecules at the W sites). Because the results obtained for the latter reaction could be interpreted in terms of either successive substitution of the different types of water coordinated at a single metal ion or of deviation from statistical kinetics, the reaction of the related $[\text{W}_3\text{S}_4(\text{H}_2\text{O})_9]^{4+}$ complex with NCS^- was reexamined, and the obtained results provide a complete picture about the relative substitution rates of the nine water molecules in these types of clusters for the first time.

Experimental Section

General Procedures and Materials. All preparations were carried out under N_2 . Stock solutions of $[\text{W}_3\text{Se}_4(\text{H}_2\text{O})_9]^{4+}$ in 2 M HCl and $[\text{W}_3\text{S}_4(\text{H}_2\text{O})_9]^{4+}$ in 2 M Hpts were prepared by the

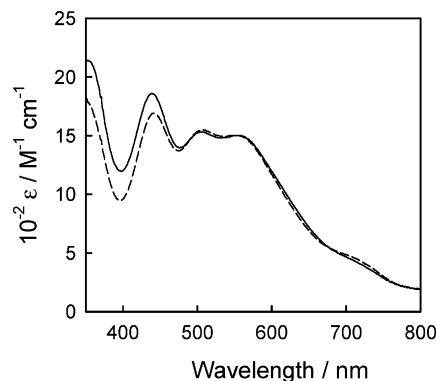


Figure 1. Electronic spectra of clusters **1Cl** in 2.0 M HCl (solid line) and **1** in 2.0 M Hpts (dashed line).

published procedures¹⁰ and purified by Dowex 50W-X2 cation-exchange chromatography. The purity of the samples was confirmed by the electronic spectra, which agree well with those previously reported in the literature.¹⁰ $\text{Pd}(\text{dba})_2$ was made as described in the literature.¹¹ Other reagents, including PdCl_2 , phenylsulfonic acid (PhSO_2H), dibenzylideneacetone, *p*-toluenesulfonic acid (Hpts), and cucurbit[6]uril (cuc), were used as purchased (Aldrich). The electronic spectra were recorded on a Shimadzu 2201 UV-vis spectrophotometer.

Preparation of the $[\text{W}_3(\text{PdCl})\text{Se}_4(\text{H}_2\text{O})_9]^{3+}$ Cationic Cluster in HCl (1Cl**).** The wine-red cuboidal cluster $[\text{W}_3(\text{PdCl})\text{Se}_4(\text{H}_2\text{O})_9]^{3+}$ was prepared in a 2.0 M HCl solution by adding a large excess of $\text{Pd}(\text{dba})_2$ to a solution of green $[\text{W}_3\text{Se}_4(\text{H}_2\text{O})_9]^{4+}$ (5 mM in 2 M HCl) and heating the mixture under N_2 under stirring for 10 h at 70 °C. Unreacted $\text{Pd}(\text{dba})_2$ was filtered off, and the product was purified by Dowex 50W-X2 cation-exchange chromatography. The solution was loaded after dilution to $[\text{H}^+] = 0.5$ M HCl. The column was washed with 100 mL of 0.50 M HCl, followed by 1.0 M HCl until the wine-red $[\text{W}_3(\text{PdCl})\text{Se}_4(\text{H}_2\text{O})_9]^{3+}$ (coming out first) clearly separated from a minor amount of the unreacted green $[\text{W}_3\text{Se}_4(\text{H}_2\text{O})_9]^{4+}$. Final elution was achieved with 2.0 M HCl. Yields were 85–95% based on the conversion of $[\text{W}_3\text{Se}_4(\text{H}_2\text{O})_9]^{4+}$, and concentrations of eluted $[\text{W}_3(\text{PdCl})\text{Se}_4(\text{H}_2\text{O})_9]^{4+}$ were in the range of 5–12 mM. The electronic spectrum of the cluster is included in Figure 1, and the UV-vis peak positions are λ/nm ($\epsilon/\text{M}^{-1}\text{cm}^{-1}$): $\epsilon_{350} = 2141$; $\epsilon_{439} = 1860$; $\epsilon_{506} = 1534$; $\epsilon_{555} = 1502$. The solutions of **1Cl** are air-sensitive. Air oxidation regenerates $[\text{W}_3\text{Se}_4(\text{H}_2\text{O})_9]^{4+}$.

Conversion of **1Cl to the Palladium Aqua Complex $[\text{W}_3(\text{Pd}(\text{H}_2\text{O}))\text{Se}_4(\text{H}_2\text{O})_9]^{4+}$ (**1**) and Isolation of the pts⁻ Salt of the Double Cube $[\text{W}_6\text{Pd}_2\text{Se}_8(\text{H}_2\text{O})_{18}]^{8+}$ (**2**).** A solution of the chloro complex $[\text{W}_3(\text{PdCl})\text{Se}_4(\text{H}_2\text{O})_9]^{3+}$ was loaded onto a Dowex 50W-X2 column and washed successively with 100 mL each of 0.5 and 1.0 M Hpts, and the resulting aqua complex **1** was eluted with 2.0 M Hpts (thus confirming the 4+ charge of the cluster aqua complex in solution). The electronic spectra of clusters **1** and **1Cl** are compared in Figure 1. Elution of concentrated solutions with 4 M Hpts from a short column allowed the crystallization of dark-red crystals of the *p*-toluenesulfonate salt $[\text{W}_6\text{Pd}_2\text{Se}_8(\text{H}_2\text{O})_{18}](\text{pts})_8 \cdot 18\text{H}_2\text{O}$ (**2a**) after storage at 4 °C for 7 days.

Preparation of the Cationic Cluster $[\text{W}_3(\text{Pd}(\text{PhSO}_2))\text{Se}_4(\text{H}_2\text{O})_9]^{3+}$ (3**) and of Its Adduct with Cucurbit[6]uril (**3a**).** To a solution of $[\text{W}_3(\text{PdCl})\text{Se}_4(\text{H}_2\text{O})_9]^{3+}$ (5 mM; 7 mL) in 2 M HCl was added 10 mg (0.07 mmol) of PhSO_2H . UV-vis: $\epsilon_{429} = 3876 \text{ M}^{-1}$

- (3) (a) Hidai, M.; Kuwata, S.; Mizobe, Y. *Acc. Chem. Res.* **2000**, *33*, 46. (b) Takei, I.; Enta, Y.; Wakabe, Y.; Suzuki, T.; Hidai, M. *Chem. Lett.* **2006**, *35*, 590. (c) Fujimura, T.; Seino, H.; Hidai, M.; Mizobe, Y. *J. Organomet. Chem.* **2004**, *689*, 738. (d) Shinozaki, A.; Seino, H.; Hidai, M.; Mizobe, Y. *Organometallics* **2003**, *22*, 4636. (e) Takei, I.; Suzuki, K.; Enta, Y.; Dohki, K.; Suzuki, T.; Mizobe, Y.; Hidai, M. *Organometallics* **2003**, *22*, 1790. (f) Masui, D.; Kochi, T.; Tang, Z.; Ishii, Y.; Mizobe, Y.; Hidai, M. *J. Organomet. Chem.* **2001**, *620*, 69. (g) Masui, D.; Ishii, Y.; Hidai, M. *Bull. Chem. Soc. Jpn.* **2000**, *73*, 931. (h) Herbst, K.; Monari, M.; Brorson, M. *Inorg. Chem.* **2001**, *40*, 2979. (i) Sokolov, M. N.; Villagra, D.; El-Hendawy, M. A.; Kwak, C.; Elsegood, M. R. J.; Clegg, W.; Sykes, A. G. *J. Chem. Soc., Dalton Trans.* **2001**, 2611. (j) Herbst, K.; Monari, M.; Brorson, M. *Inorg. Chem.* **2002**, *41*, 1336. (k) Herbst, K.; Zanello, P.; Corsini, M.; Damelio, N.; Dahlenburg, L.; Brorson, M. *Inorg. Chem.* **2003**, *42*, 974. (l) Takei, I.; Wakebe, Y.; Suzuki, K.; Enta, Y.; Suzuki, T.; Mizobe, Y.; Hidai, M. *Organometallics* **2003**, *22*, 4639. (m) Takei, I.; Suzuki, K.; Enta, Y.; Dohki, K.; Suzuki, T.; Mizobe, Y.; Hidai, M. *Organometallics* **2003**, *22*, 1790. (n) Geiger, W. E.; Ohrenberg, N. C.; Yeomans, B.; Connelly, N. G.; Emslie, D. J. *H. J. Am. Chem. Soc.* **2003**, *125*, 8680. (o) Takei, I.; Dohki, K.; Kobayashi, K.; Suzuki, T.; Hidai, M. *Inorg. Chem.* **2005**, *44*, 3768. (p) Akashi, H.; Isobe, K.; Shibahara, T. *Inorg. Chem.* **2005**, *44*, 3494. (q) Feliz, M.; Llusar, R.; Uriel, S.; Vicent, C.; Brorson, M.; Herbst, K. *Polyhedron* **2005**, *10*, 1212.
- (4) (a) Algarra, A. G.; Basallote, M. G.; Fernandez-Trujillo, M. J.; Hernandez-Molina, R.; Safont, V. S. *Chem. Commun.* **2007**, 29, 3071.
- (5) (a) Sokolov, M.; Virovets, A.; Dybtsev, D.; Chubarova, E.; Fedin, V.; Fenske, D. *Inorg. Chem.* **2001**, *40*, 4816. (b) Sokolov, M. N.; Chubarova, E. V.; Virovets, A. V.; Llusar, R.; Fedin, V. P. *J. Cluster Sci.* **2003**, *14*, 227.
- (6) Murata, T.; Gao, H.; Mizobe, Y.; Nakano, F.; Motomura, S.; Tanase, T.; Yano, S.; Hidai, M. *J. Am. Chem. Soc.* **1992**, *114*, 8287.
- (7) (a) Murata, T.; Mizobe, Y.; Gao, H.; Ishii, Y.; Wakabayashi, T.; Nakano, F.; Tanase, T.; Yano, S.; Hidai, M.; Echizen, I.; Nanikawa, H.; Motomura, S. *J. Am. Chem. Soc.* **1994**, *116*, 3389. (b) Wakabayashi, T.; Ishii, Y.; Ishikawa, K.; Hidai, M. *Angew. Chem., Int. Ed. Engl.* **1996**, *35*, 2123. (c) Wakabayashi, T.; Ishii, Y.; Murata, T.; Mizobe, Y.; Hidai, M. *Tetrahedron Lett.* **1995**, *36*, 5585.
- (8) Fedin, V. P.; Seo, M. S.; Saysell, D. M.; Dybtsev, D. N.; Elsegood, M. R. J.; Clegg, W.; Sykes, A. G. *J. Chem. Soc., Dalton Trans.* **2002**, 138.
- (9) Hernandez-Molina, R.; Kalinina, I.; Sokolov, M.; Clausen, M.; Platas, J. G.; Vicent, C.; Llusar, R. *Dalton Trans.* **2007**, 550.

- (10) Fedin, V. P.; Sokolov, M. N.; Virovets, A. V.; Podberezhskaya, N. V.; Fedorov, V. Y. *Inorg. Chim. Acta* **1998**, *269*, 292.
- (11) Rettig, M. F.; Maitlis, P. M. *Inorg. Synth.* **1990**, *28*, 110.

cm⁻¹. Single crystals of [W₃(Pd(PhSO₂))Se₄(H₂O)_{8.58}Cl_{0.42}]₂·(C₃₆H₃₆N₂₄O₁₂)Cl_{5.16}·16.83H₂O (**3a**) were further isolated from this solution as a supramolecular adduct with cucurbit[6]uril. To achieve this, 1 mL of a saturated solution of cucurbit[6]uril in 4 M HCl was added to 1 mL of the resulting solution of **3**. Red-brown crystals of **3a** separated overnight. Anal. Calcd for C₄₈H₁₁₄Cl₆N₂₄O₅₀·Pd₂S₂Se₈W₆: C, 14.21; H, 2.8; N, 8.3; S, 1.6. Found: C, 14.8; H, 3.61; N, 8.6; S, 1.2.

Solution Studies on the Reactivity of Clusters 1 and 1Cl, Including the Stabilization of Pyramidal Tautomers of H₃PO₂ and H₃PO₃ by Coordination to the Heterometal. Solution studies were carried out to check the reactivity of cluster **1** with a variety of substrates. The reagents used for this purpose were H₃PO₃, H₃PO₂, and As(OH)₃.

To a solution of [W₃(PdCl)Se₄(H₂O)₉]³⁺ (5 mM; 7 mL) in 2 M HCl was added H₃PO₃ (10 mg) or H₃PO₂ (3 drops of a 50% aqueous solution). The wavelengths and molar absorptivities of new bands in the UV-vis spectra ($\epsilon_{415} = 3260 \text{ M}^{-1} \text{ cm}^{-1}$ for the HP(OH)₂ complex and $\epsilon_{424} = 3820 \text{ M}^{-1} \text{ cm}^{-1}$ for the P(OH)₃ complex) agree well with those reported for [W₃(Ni(HP(OH)₂))Se₄(H₂O)₉]⁴⁺ and [Mo₃(Pd(P(OH)₃)S₄(H₂O)₆Cl₃)]⁴⁺ containing these tautomers. The reaction of an excess of As₂O₃ with [W₃PdSe₄(H₂O)₁₀]⁴⁺ is rapid and produces spectral changes attributable to the formation of the As(OH)₃ complex⁹ ($\epsilon_{425} = 4084.15 \text{ M}^{-1} \text{ cm}^{-1}$). No spectral changes were observed upon the addition of Sb₂O₃.

X-ray Crystallography. Diffraction data were collected at room temperature on a Bruker-Nonius Kappa CCD diffractometer with graphite-monochromated Mo K α radiation ($\lambda = 0.71073 \text{ \AA}$). Frames were collected with the *Collect* program¹² and indexed and processed with *Denzo SMN*, and the files were scaled together with the *HKL2000* program.¹³ The absorption correction was applied with a semiempirical method based on multiple scanned reflections by means of the *PLATON* program.¹⁴ The structure was solved by direct methods using the *SIR2004* program¹⁵ and refined using the *SHELXL-97* program.¹⁶ All non-H atoms were refined with anisotropic thermal parameters using full-matrix least-squares procedures on F^2 . H atoms were refined as rigid groups except those from water molecules, which were not included in the refinement. Crystallographic data and data collection details are given in Table 1. The crystallographic data have been deposited in the Cambridge Crystallographic Data Center under deposition codes CCDD 708229 for (**2a**) and 708230 for (**3a**).

Kinetic Studies. The kinetic experiments were carried out with an Applied Photophysics SX17MV stopped-flow spectrometer provided with a PDA1 photodiode array detector. All experiments were carried out under N₂ under pseudo-first-order conditions of ligand excess at 25.0 °C by mixing aqueous solutions of the corresponding cluster (**1** or [W₃S₄(H₂O)₉]⁴⁺) with a solution containing an excess of H₃PO₂ or KSCN in 2 M Hpts. For the reaction of [W₃S₄(H₂O)₉]⁴⁺ with thiocyanate, kinetic experiments were also made at Hpts concentrations of 1.0 and 0.5 M, with the ionic strength being maintained as 2.0 M with Lipts. The concentration of the cluster solutions was $2.4 \times 10^{-3} \text{ M}$ in the case of **1** and

Table 1. Crystallographic Data for **2a** and **3a**

compound	2a	3a
empirical formula	C ₅₆ H ₁₂₈ O ₆₀ Pd ₂ S ₈ Se ₈ W ₆	C ₄₈ H ₁₁₄ Cl ₆ N ₂₄ O ₅₀ Pd ₂ S ₂ Se ₈ W ₆
fw	3965.64	4051.95
cryst syst	triclinic	orthorhombic
<i>a</i> , Å	11.7366(9)	21.1201(6)
<i>b</i> , Å	15.0088(14)	22.1594(9)
<i>c</i> , Å	16.4770(16)	23.944(1)
α , deg	77.862(5)	90
β , deg	84.503(5)	90
γ , deg	82.573(5)	90
<i>V</i> , Å ³	2806.7(4)	11206.0(7)
<i>T</i> , K	293(2)	293(2)
space group	<i>P</i> $\bar{1}$	<i>Pbca</i>
<i>Z</i>	1	4
μ (Mo K α), mm ⁻¹	9.268	9.318
reflns collected	50 096	88 502
ϕ range for data collection	1.3–28.7	2.1–27.5
unique reflns/ <i>R</i> _{int}	13 819/0.086	12 335/0.089
GOF on F^2	1.00	1.12
<i>R</i> ¹ / <i>wR</i> ² ^b	0.0452/0.1001	0.0621/0.1581
<i>R</i> ¹ / <i>wR</i> ² ^b (all data)	0.0926/0.1457	0.0876/0.1710
residual ρ , e Å ⁻³	+1.82 and -2.93	+2.12 and -2.44

$$^a R1 = \sum |F_o| - |F_c| / \sum F_o. \quad ^b wR2 = [\sum (w(F_o^2 - F_c^2))^2 / \sum (w(F_o^2)^2)]^{1/2}.$$

$3.4 \times 10^{-3} \text{ M}$ in the case of [W₃S₄(H₂O)₉]⁴⁺, and the concentration of the entering ligand was changed within the ranges shown in the Results and Discussion section. In all cases, kinetic data at multiple wavelengths were analyzed with the *Specfit* program¹⁷ using the kinetic models indicated in the corresponding section.

Results and Discussion

Synthesis of the W₃PdSe₄ Clusters. In a sharp contrast to the smooth reaction of [Mo₃Q₄(H₂O)₉]⁴⁺ (Q = S, Se) with Pd black, [W₃(PdCl)Se₄(H₂O)₉]³⁺ cannot be accessed by the direct incorporation of Pd into [W₃Se₄(H₂O)₉]⁴⁺, and it was prepared by reaction of the latter with Pd(dba)₂ as the Pd⁰ source. The reaction of [W₃Se₄(H₂O)₉]⁴⁺ with PdCl₂ and hypophosphorous acid as the reducing agent did not lead to [W₃(PdCl)Se₄(H₂O)₉]³⁺, in contrast to the reaction with the analogous W₃S₄ cluster. Pd₂(dba)₃ was used as the Pd⁰ source in the preparation of [Mo₃(Pd(dppe))S₄(dppe)₃Cl₃]⁺ from [Mo₃S₄(H₂O)₉]⁴⁺, dppe, and Pd₂(dba)₃.¹⁸ Like in the case of the other [W₃(MCl)Q₄(H₂O)]³⁺ clusters (M = Ni, Pd; Q = S, Se), decomplexation of Cl⁻ from the heterometal leads (via the intermediate aqua complex, [W₃(M(H₂O))Q₄(H₂O)]⁴⁺) to the edge-linked double-cuboidal clusters [(W₃MQ₄(H₂O)₉]₂)⁸⁺, where the fourth coordination site of the tetrahedrally coordinated M is occupied by one of the chalcogen atoms of the “twin” cuboidal unit. This interconversion is fully reversible. In 1–2 M HCl, the dominant species is likely to be **1Cl**. The 3+ charge can be deduced from the column behavior because it is eluted before the tetrapositive [W₃Se₄(H₂O)₉]⁴⁺. In a Hpts solution, the cluster must be present as **1** because it is readily eluted with 2 M Hpts. However, from refrigerated concentrated solutions eluted with 4 M Hpts, only the edge-linked double-cuboidal cluster [(W₃PdSe₄(H₂O)₉]₂(pts)₈·18H₂O crystallizes. Solutions of both **1** and **1Cl** are air-sensitive in solutions and must be stored under N₂.

(12) Bruker-Nonius (1997–2000): *Collect Program Suite*; Bruker-Nonius: Dordrecht, The Netherlands, 1997–2000.

(13) Otwinowski, Z.; Minor, W. In *Processing of X-ray Diffraction Data Collected in Oscillation Mode*; Carter, C. W., Jr., Sweet, R. M., Eds.; Macromolecular Crystallography; Academic Press: New York, 1997; Vol. 276, part A, pp 307–326.

(14) Spek, A. L. *Acta Crystallogr.* **1990**, *A46*, C34.

(15) Burla, M. C.; Caliandro, R.; Camalli, M.; Carrozzini, B.; Cascarazo, G. L.; De Caro, L.; Giacovazzo, C.; Polidori, G.; Spagna, R. *J. Appl. Crystallogr.* **2005**, *38*, 381.

(16) Sheldrick, G. M. *SHELXL-97, Program for the refinement of Crystal Structures*; University of Göttingen; Göttingen, Germany, 1997.

(17) Binstead, R. A.; Jung, B.; Zuberbühler, A. D. *SPECFIT-32*; Spectrum Software Associates: Chapel Hill, NC, 2000.

(18) Masai, D.; Ishii, Y. *Bull. Chem. Soc. Jpn.* **2000**, 931.

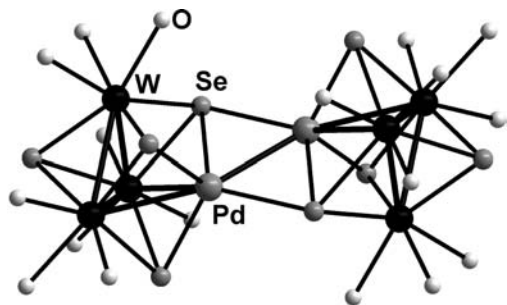


Figure 2. View of the $[W_6Pd_2Se_8(H_2O)_{18}]^{8+}$ cluster in **2a**.

The addition of S-, P-, or As-containing ligands to a solution of **1Cl** in 2 M HCl produces color changes and spectral shifts typical of the replacement of Cl^- at Pd with the formation of $[W_3(PdL)Se_4(H_2O)_9]^{4+}$ ($L = PhSO(O)^-$, $HP(OH)_2$, $P(OH)_3$, $As(OH)_3$). Some representative examples of these spectral changes are included in the Supporting Information. The reaction leads in all cases to the appearance of an intense absorption band centered at the wavelengths listed in the Experimental Section, close to the positions found for other clusters containing the same ligands.^{5a,20} The reaction of $PhSO(O)^-$ and $As(OH)_3$ with $[W_3(PdL)Se_4(H_2O)_9]^{4+}$ is very fast, and their kinetics could not be followed by stopped-flow techniques. The reaction with phosphorous acids is much slower. The driving force for these reactions must be the high affinity of low-valence Pd for the soft donors (P, As, S). According to the criteria commonly established in the literature, the metal oxidation states in the cluster core can be assigned as $W^{IV}_3Pd^0$,^{8,19} and the affinity of tetrahedral Pd^0 for the phosphines is well-known. The coordination of the Pd atom through the P atom must involve the isomerization of $H_2P(O)(OH)$ and $HP(O)(OH)_2$ into $HP(OH)_2$ and $P(OH)_3$, respectively, to create the lone pair at the P atom and to make thus the coordination possible: $H_2P(O)(OH) \rightarrow HP(OH)_2$; $HP(O)(OH)_2 \rightarrow P(OH)_3$.

To obtain single crystals of the phenylsulfinate complex **3**, a solution of the macrocyclic cavitand cucurbit[6]uril in 4 M HCl was added to the reaction solution to induce the formation of complementary supramolecular associates, isolated as **3a**.²⁰

X-ray structure analysis of **3a** reveals the presence of the double-cuboidal core $\{W_3PdSe_4\}_2^{8+}$ in which the Pd atoms are bridged by two μ_4 -Se atoms [Se(1)] with the intracuster Pd–Se(1) distance of 2.606(1) Å and the intercluster Pd–Se(1') distance of 2.537(1) Å and with a short Pd–Pd bond of 2.764(2) Å (Figure 2). It should be noted that the Pd–Pd distance shows little variation with M and Q in the whole $[M_6Pd_2Q_8(H_2O)_{18}]^{8+}$ series (Table 2). The rhombus Pd_2Se_2 is strictly planar. The two Pd– μ_3 -Se bonds are shorter, 2.462–2.465 Å. Similar cluster units $\{M_3M'Q_4\}_2^{8+}$ ($M = Mo, W$; $M' = Ni, Pd$; $Q = S, Se$) are observed in the corresponding aqua complexes $[W_6Ni_2Q_8(H_2O)_{18}](p-CH_3C_6-$

$H_4SO_3)_8 \cdot nH_2O$ (Table 2). A center of symmetry resides on the midpoint of the two Pd atoms. Each edge-linked cluster core consists of a distorted tetrahedral arrangement of one Pd atom and three W atoms. The Pd–W distances are 2.8911(9) Å (W1–Pd), 2.7623(9) Å (W2–Pd), and 2.8365(8) Å (W3–Pd), thus defining a very distorted tetrahedral cluster unit W_3Pd . Each W atom is coordinated to three terminal water molecules and three Se bridging ligands in an octahedral environment, while the Pd atoms are in a tetrahedral disposition defined by four Se atoms if the metal–metal bonds are ignored. The incorporation of Pd into the incomplete cuboidal unit slightly lengthens the W–W distances.

The 2:1 supramolecular cucurbit[6]uril adduct **3a** crystallizes in the *Pbca* space group with cell parameters very close to those reported for $\{[W_3(Pd(PhP(OH)_2)S_4(H_2O)_7-Cl_2)Cl_2]_2(C_{36}H_{36}N_{24}O_{12}) \cdot 9.5H_2O\}$,⁹ which is not surprising taking into account the fact that $PhSO(OH)$ and $PhP(OH)_2$ are isoelectronic and have very similar geometry. From the nonintegral composition of **3a**, it can be deduced that both $[W_3(Pd(PhSO_2))Se_4(H_2O)_9]^{3+}$ and $[W_3(Pd(PhSO_2))Se_4(H_2O)_8Cl]^{2+}$ are present in the same crystal. Figure 3 shows the structure of the cationic supramolecular complex $\{[W_3(Pd(PhSO_2))S_4(H_2O)_8Cl]_2^{4+}(C_{36}H_{36}N_{24}O_{12})\}$ in the crystal of **3a**. The geometry of the cluster core is analogous to that observed in the edge-linked subunits in the $\{W_3PdSe_4\}_2^{8+}$ cluster of **2a** except that the outer position at Pd is occupied by the S atoms of the $PhSO_2^-$ ligand. The coordination environment around each W is mostly filled by three water molecules. In one of the positions, namely, that at W(2), which can be named syn with respect to the orientation of the $PhSO_2$ group at the neighboring Pd atom, the occupancy is 52% H_2O and 48% Cl . The Cl/H_2O occupancy in the cluster was refined by fixing the full occupancy of the site as 1 and varying the Cl/H_2O ratio until reasonable thermal parameters were obtained. The other positions were regarded as occupied only by coordinated water molecules, based on the analysis of bond distances and thermal parameters. The overall charge was balanced with $6Cl^-$ as required for the electroneutrality, taking into account the presence of two cluster units $W_3PdSe_4^{4+}$ and two $PhSO_2^-$ ligands.

The coordination site at Pd is occupied by deprotonated $PhSO_2^-$ ligand [two S–O bonds of 1.481(9) and 1.490(8) Å, S–C of 1.80(1) Å, two O–S–C angles of 102.2(5)° and 102.7(5)°, and an O–S–O angle of 110.9(5)°]. Thus, $PhSO_2^-$ is less “pyramidal” and more “tetrahedral” than $PhP(OH)_2$ in $[W_3(Pd(PhP(OH)_2)S_4(H_2O)_8)Cl]^{2+}$.⁹ The Pd–S bond is 2.296(3) Å, and the Se–Pd–S angles are 108–116°. The phenyl ring plane is almost orthogonal to the Mo_3 plane in the cluster and is oriented in such a way as to be almost coplanar with one of the Pd–Mo bonds, to give a chiral rotamer.

Six water molecules in the cis position to the μ_3 -Se ($-W_3$) atom form hydrogen bonds with portal O atoms of cucurbituril ($O \cdots O$ of 2.7–3.0 Å), giving a discrete “two lids on the barrel” type units $\{W_3Pd\}-(cuc)-\{W_3Pd\}$ (Figure 3). According to the 2:1 stoichiometry of the compound, the

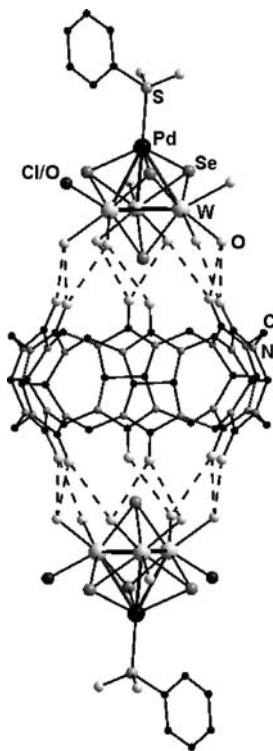
(19) Sells, D. M.; Lamprecht, G. J.; Darkwa, J.; Sykes, A. G. *Inorg. Chem.* **1996**, *35*, 5531.

(20) Sokolov, M. N.; Hernández-Molina, R.; Dybtsev, D.; Chubarova, E. V.; Solodovnikov, S. F.; Pervukhina, N. V.; Vicent, C.; Llusar, R.; Fedin, V. P. *Z. Anorg. Allg. Chem.* **2002**, *628*, 2335.

Table 2. Comparison of Main Geometric Parameters (Å) for the Edge-Linked Double-Cuboidal Clusters [M₆M′₂Q₈(H₂O)₁₈]⁸⁺ (M = Mo, W; M′ = Ni, Pd; Q = S, Se)

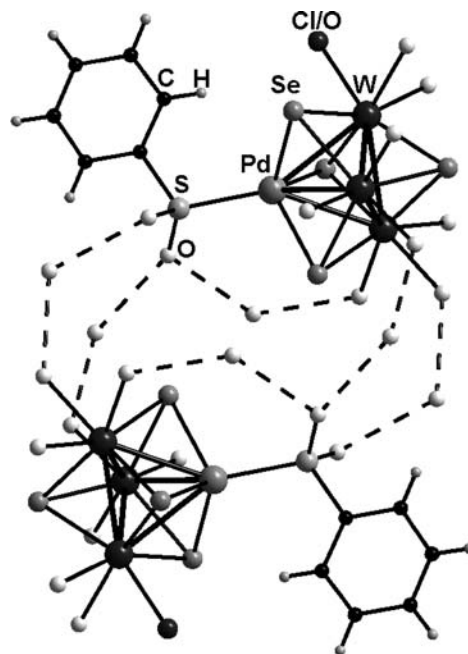
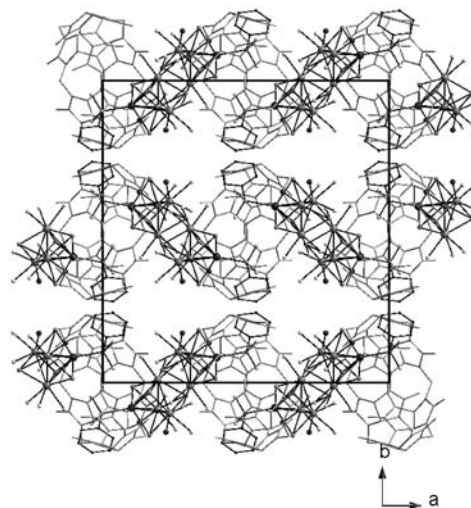
cluster	M–M	M–M′	M′–M′	M′–μ ₄ Q ^a	ref
[W ₆ Ni ₂ S ₈ (H ₂ O) ₁₈] ⁸⁺	2.726(1)–2.746(1)	2.613(3)–2.698(4)	2.561(5)	2.56(6), 2.257(6)	33
[W ₆ Ni ₂ Se ₈ (H ₂ O) ₁₈] ⁸⁺	2.749(2)–2.815(1)	2.652(2)–2.741(3)	2.570(3)	2.375(3), 2.386(2)	34
[Mo ₆ Pd ₂ S ₈ (H ₂ O) ₁₈] ⁸⁺	2.759(1)–2.789(1)	2.746(1)–2.836(1)	2.790(1)	2.414(2), 2.502(2)	8
[Mo ₆ Pd ₂ Se ₈ (H ₂ O) ₁₈] ⁸⁺	2.7953(6)–2.8650(6)	2.7459(6)–2.8556(6)	2.749(6)	2.5350(6), 2.5673(6)	11
[W ₆ Pd ₂ S ₈ (H ₂ O) ₁₈] ⁸⁺	2.7237(9)–2.7385(9)	2.726–2.852	2.752(2)	2.425(7), 2.56(2)	9
[W ₆ Pd ₂ Se ₈ (H ₂ O) ₁₈] ⁸⁺	2.761(5)–2.819(4)	2.762–2.891	2.764(8)	2.537(4), 2.606(8)	this work

^a The intercluster distance (first value) and intracenter distance (second value) are given.

**Figure 3.** View of the 2:1 supramolecular adduct of W₃(Pd(PhSO₂))Se₄(H₂O)₈-Cl]²⁺ with cucurbituril in **3a**.

two portals of the cucurbituril macrocycle are closed by the [W₃(Pd(PhSO₂))S₄(H₂O)₈Cl]²⁺ or [W₃(Pd(PhSO₂))S₄(H₂O)₉]³⁺ cations, as shown in Figure 4. These associates are held together by additional water molecules, which participate in hydrogen bonding involving two aqua ligands of one cluster cation, the two O atoms of the phenylsulfonic ligand at a neighboring cluster, and two water molecules connecting them together. In this way dimeric associates arise (Figure 5). Besides, one of the O atoms of the coordinated sulfonic acid and one of the coordinated water molecules are involved in hydrogen bonding with the same water molecule [O⋯O(S) of 2.77(1) Å and O⋯O(W) of 2.60(1)] Å so that a bridging “chelate” ring SOOO forms on one of the Pd–W bonds.

Kinetic Studies. One of the most interesting aspects of the reactivity of metal clusters is the possibility of exploring the reactivity changes associated with the close proximity of several metal centers. In particular, the M₃M′Q₄ clusters contain two types of metal centers, and they allow detailed and systematic studies of the changes in the reactivity associated with the M–M′ interactions, depending on both M and M′. Previous studies on these kinds of complexes, in general, indicate that the kinetics of substitution reactions

**Figure 4.** View of the supramolecular dimeric unit {[W₃(Pd(PhSO₂))Se₄(H₂O)₈Cl]₂(H₂O)₆]⁴⁺.**Figure 5.** Packing in the crystal of **3a**.

at both types of atoms can be easily separated, with substitutions at M′ usually running faster than they do at M (M = Mo, W).^{1,19} This is the case of the Mo₃PdS₄ clusters, for which the first report on kinetics¹⁹ indicated that substitution reactions at Pd are several orders of magnitude faster than the reactions at Mo when the entering ligand is a halide or thiocyanate and that the reaction occurs exclusively at the Pd site when the entering ligand is a soft,

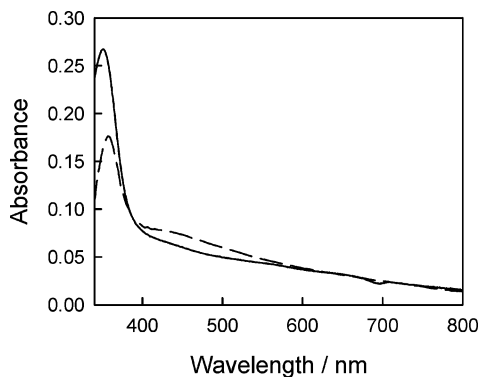


Figure 6. Comparison between the electronic spectrum obtained immediately upon mixing in the stopped-flow instrument solutions of **1** and NCS^- (dashed line) and the spectrum calculated by averaging the spectra measured for the separate solutions (solid line).

π -acceptor ligand like CO or a phosphine. More recently, we have conclusively demonstrated⁴ that the stabilization of the pyramidal tautomer of H_3PO_2 occurs at the Pd site without any evidence of a competing complexation to Mo, a finding further supported by the solution studies carried out in the present work. In this work, we have tried to obtain additional information about the kinetics of reaction of these clusters by examining processes occurring at both types of metal centers in new cluster **1**.

Kinetics of Reaction at the Pd Site of 1. The spectrum obtained immediately upon mixing in the stopped-flow instrument a solution of **1** with an excess of thiocyanate in the presence of 2.0 M Hpts does not coincide with that calculated from the spectra of both solutions (see Figure 6), thus showing a rapid reaction that occurs within the mixing time of the instrument and so no values of the observed rate constant for this step ($k_{1\text{obs}}$) could be measured. These very rapid changes are followed by slower changes occurring in the stopped-flow time scale, which most likely correspond to substitution at the W sites and which will be discussed in the next section. At this point, the focus will be made exclusively upon the initial change shown in Figure 6, which can be tentatively assigned as corresponding to substitution of the water coordinated at the Pd center by entering SCN^- , as was reported for the related Mo_3PdS_4 complex.¹⁹ Actually, we have been unable to monitor the kinetics of very fast reactions with other entering ligands that coordinate exclusively at Pd, such as the reaction of **1** with PhSO_2H leading to the formation of **3**. These observations confirm that, as expected, the Pd site of **1** is much more labile than the W centers.

However, although we have been unable to obtain details about the kinetics of substitution at the Pd site of **1** when the entering ligand is thiocyanate, the kinetics of reaction with H_3PO_2 could be studied in detail. The spectral changes attributable to the formation of $[\text{W}_3(\text{Pd}(\text{HP}(\text{OH})_2))\text{Se}_4]^{4+}$ in 2.0 M Hpts clearly reveal biphasic kinetics (see Figure 7), which indicates the existence of a detectable reaction intermediate. As occurred in the case of the Mo_3PdS_4 complex,⁴ the spectrum calculated from the kinetic data for the reaction intermediate is very similar to that of the starting complex, whereas the second kinetic step occurs with much

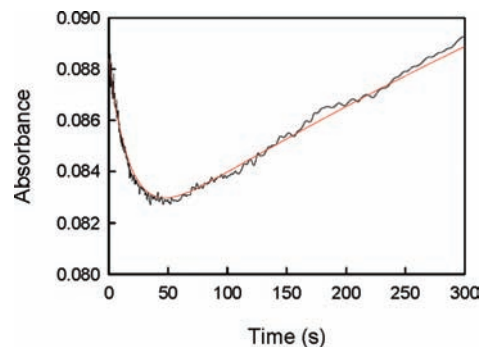


Figure 7. Kinetic trace at 363 nm showing the biphasic kinetics in the reaction of cluster **1** with H_3PO_2 .

larger absorbance changes associated with the evolution of the band at 415 nm for the reaction product. These results can be interpreted in a way similar to that for the molybdenum analogue by considering that the first resolved kinetic step consists of substitution at the Pd center to form an intermediate with O-coordinated tetrahedral H_3PO_2 and that the second step corresponds to tautomerization of the coordinated H_3PO_2 . However, whereas in the case of the molybdenum complex both kinetic steps show a first-order dependence on $[\text{H}_3\text{PO}_2]$, in the case of **1**, both rate constants are independent of $[\text{H}_3\text{PO}_2]$, with their values being $k_{1\text{obs}} = (6.8 \pm 0.8) \times 10^{-2} \text{ s}^{-1}$ and $k_{2\text{obs}} = (1.3 \pm 0.3) \times 10^{-3} \text{ s}^{-1}$. Nevertheless, these results can still be interpreted within the previously proposed mechanism. Thus, in the first resolved kinetic step, the substitution must go through the rapid formation of an outer-sphere complex (eq 1) followed by rate-determining expulsion of water by the entering ligand, the O-coordinated H_3PO_2 (eq 2), so that the values of the observed rate constant are expected to show a saturation behavior at increasing $[\text{H}_3\text{PO}_2]$. The observation of rate constants independent of $[\text{H}_3\text{PO}_2]$ would thus indicate the formation of a very stable outer-sphere complex, a behavior not very surprising given the ability of phosphorous acids to form strong hydrogen bonds.²¹ According to the previously proposed mechanism,⁴ the second resolved kinetic step would correspond to the isomerization of the coordinated H_3PO_2 in a process (eqs 3–5) assisted by a second H_3PO_2 molecule, which catalyzes a hydrogen shift from P to O in the O-coordinated H_3PO_2 , thus leading to the formation of an intermediate containing O-coordinated pyramidal $\text{HP}(\text{OH})_2$ (eqs 3 and 4). In the next step, this intermediate rearranges to give the final reaction product (eq 5). Density functional theory calculations indicated that for the Mo_3PdS_4 complex the second resolved kinetic step is controlled by proton abstraction (eq 3), which results in first-order dependence on $[\text{H}_3\text{PO}_2]$. However, if the rate-determining step for the second resolved step in our case displaces from eq 3 to eq 5, the observed rate constant would be independent of $[\text{H}_3\text{PO}_2]$, as observed for the reaction of **1**. As a summary, although the data available do not provide information about the reasons leading to these changes in the rate law for both steps when changing the complex from Mo_3PdS_4 to **1**, the

(21) (a) Gonzalez, L.; Mo, O.; Yanez, M.; Elguero, J. *J. Phys. Chem.* **1998**, *109*, 2685. (b) Tokhadze, K. G.; Denisov, G. S.; Wierzejewska, M.; Drozd, M. *J. Mol. Struct.* **1997**, *404*, 55.

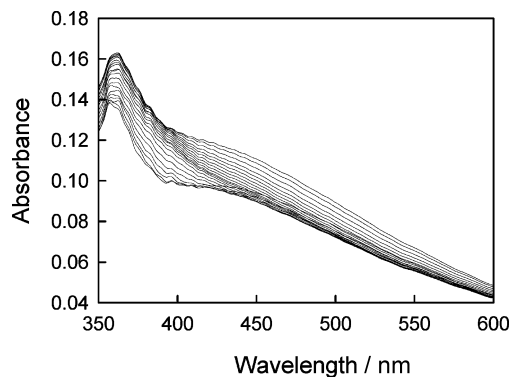
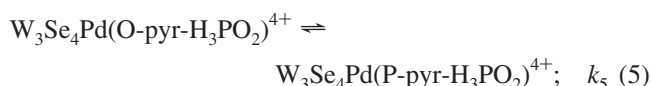
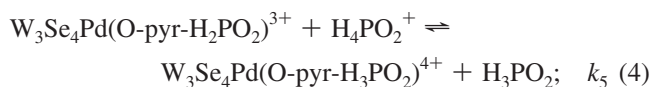
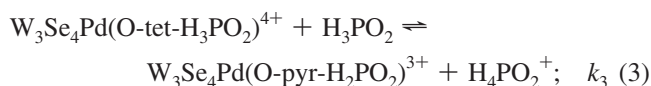
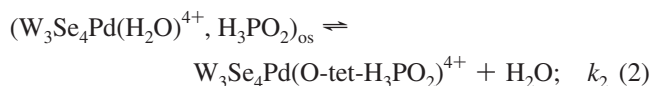
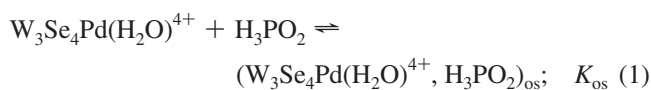


Figure 8. Typical spectral changes observed during the reaction of cluster **1** with SCN⁻ in 2.0 M Hpts. A total of 500 spectra were acquired during 1000 s with a logarithmic time base, although only some of the spectra are plotted for simplicity.

information available at this time confirms the biphasic nature of the process, and the similarity of the electronic spectra adds further support to the O-coordinated nature of the detectable reaction intermediate.



Kinetics of Reaction at the W Sites of 1. As pointed out above, following the very rapid initial absorbance changes occurring within the mixing time, stopped-flow monitoring of the kinetics of reaction of **1** with SCN⁻ allows the observation of slower absorbance changes, which are illustrated in Figure 8. A satisfactory fit of these changes requires a kinetic model with four consecutive exponentials (eq 6), and the spectra calculated for all of the colored species participating in the reaction are shown in Figure 9. With regard to the observed rate constants, those corresponding to the first three steps show a linear dependence with respect to [SCN⁻] (eq 7 and Figure 10), whereas the rate of the fourth resolved step is independent of the thiocyanate concentration. The numerical values derived for all of the rate constants are $k_{2f} = 156 \pm 4 \text{ M}^{-1} \text{ s}^{-1}$, $k_{2r} = 0.44 \pm 0.03 \text{ s}^{-1}$, $k_{3f} = 43 \pm 2 \text{ M}^{-1} \text{ s}^{-1}$, $k_{3r} = 0.04 \pm 0.01 \text{ s}^{-1}$, $k_{4f} = 3.9 \pm 0.2 \text{ M}^{-1} \text{ s}^{-1}$, $k_{4r} = 4 \pm 2 \text{ s}^{-1}$, and $k_5 = (4 \pm 1) \times 10^{-3} \text{ s}^{-1}$. Both types of rate laws have been previously observed in the kinetics of substitution reactions at M₃Q₄ and M₃M'Q₄ clusters. The linear dependence in eq 7 is typical of reversible equilibria, with the values of k_{if} corresponding to the forward substitu-

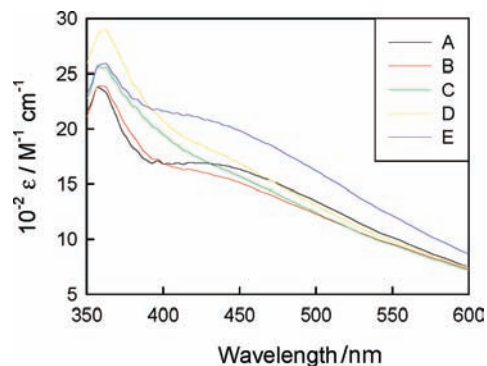


Figure 9. Spectra calculated by fitting the spectral changes in Figure 8 to a kinetic model with four consecutive exponentials. The nomenclature of the different species follows that in eq 6.

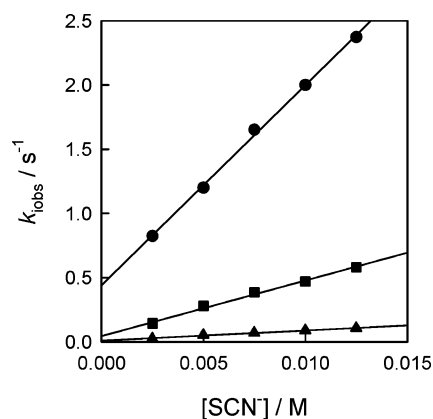
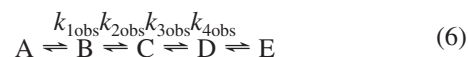


Figure 10. Plots showing the linear dependence of $k_{2\text{obs}}$ (●), $k_{3\text{obs}}$ (■), and $2k_{4\text{obs}}$ (▲) with respect to the entering ligand concentration in the reaction of cluster **1** with SCN⁻ (25.0 °C, 2.0 M Hpts).

tion and those of k_{ir} to the reverse aquation processes.^{22–24} On the other hand, rate constants independent of the concentration of the entering ligand are attributed to isomerization from S-bonded to N-bonded thiocyanate.^{1,25}



$$k_{\text{obs}} = k_{if}[\text{SCN}^-] + k_{ir} \quad (7)$$

With regard to the actual values of the rate constants, no comparison can be made with the related [W₃Se₄(H₂O)₉]⁴⁺ cluster because, although its reactivity has been explored in the preparative way,²⁶ no kinetic studies have been made on its substitution reactions. For this reason, the most direct comparison can only be made with substitution in the

- (22) (a) Kathirgamanathan, P.; Soares, A. B.; Richens, D. T.; Sykes, A. G. *Inorg. Chem.* **1985**, *24*, 2950. (b) Richens, D. T.; Helm, L.; Pittet, P. A.; Merbach, A. E.; Nicolo, F.; Chapuis, G. *Inorg. Chem.* **1989**, *28*, 1394.
- (23) Ooi, B. L.; Sykes, A. G. *Inorg. Chem.* **1988**, *27*, 310.
- (24) Ooi, B.-L.; Sykes, A. G. *Inorg. Chem.* **1989**, *28*, 3799.
- (25) Li, Y. J.; Nasreldin, M.; Humanes, M.; Sykes, A. G. *Inorg. Chem.* **1992**, *31*, 3011.
- (26) (a) Fedin, V. P.; Lamprecht, G. J.; Kohzuma, T.; Clegg, W.; Elsegood, M. R. J.; Sykes, A. G. *J. Chem. Soc., Dalton Trans.* **1997**, 1747. (b) Hernandez-Molina, R.; Dybtsev, D. N.; Fedin, V. P.; Elsegood, M. R. J.; Clegg, W.; Sykes, A. G. *Inorg. Chem.* **1998**, *37*, 2995. (c) Seo, M. S.; Fedin, V. P.; Sokolov, M. N.; Hernandez-Molina, R.; Sokolowski, A.; Elsegood, M. R. J.; Clegg, W.; Sykes, A. G. *Inorg. Chem.* **2001**, *40*, 6115. (d) Hernandez-Molina, R.; Elsegood, M. R. J.; Clegg, W.; Sykes, A. G. *J. Chem. Soc., Dalton Trans.* **2001**, 2173.

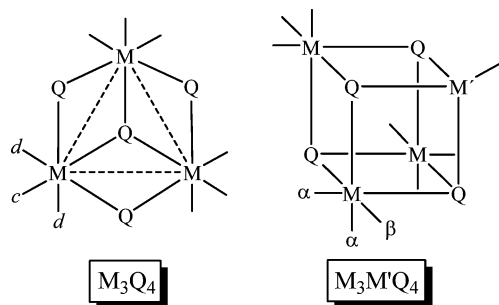


Figure 11. Structure of M_3Q_4 and $M_3M'Q_4$ clusters showing the different types of water molecules coordinated at each metal center.

Mo_3PdS_4 cluster, although care must be taken even in this case because the measured rates correspond to substitution at different metal centers (Mo or W). Sykes and co-workers were able to resolve¹⁹ the values of k_{2f} ($17\text{ M}^{-1}\text{ s}^{-1}$), k_{3f} ($0.2\text{ M}^{-1}\text{ s}^{-1}$), and an SCN^- -independent rate constant of 0.015 s^{-1} that would be equivalent to k_5 in the present work. A very rapid absorbance change occurring within the mixing time of the stopped-flow instrument and assigned to substitution at Pd was also observed in that case (k_1 step). A comparison of the values of k_{2f} and k_{3f} for both complexes indicates that changing from a cluster containing the Pd center linked to a Mo_3S_4 subunit to another one containing W_3Se_4 increases the rate of substitution at the M centers by a factor of 9 (k_{2f}) or 215 (k_{3f}), whereas the isomerization rate is reduced by a factor of ca. 4. Especially surprising appears to be the change in the factor from 9 to 215 for the increase of k_{if} , which is caused by closeness of the values of k_{2f} and k_{3f} in the case of cluster **1**.

M_3Q_4 and $M_3M'Q_4$ clusters contain two types of water molecules coordinated at the M centers.^{1,19} Following the notations of Sykes, these water molecules are labeled as *c* (trans to μ_3 -Q) and *d* (trans to μ_2 -Q) in M_3Q_4 clusters and β and α in $M_3M'Q_4$ clusters, respectively (see Figure 11). Although there is a simple correlation between them ($c = \beta$ and $d = \alpha$), this change in the nomenclature is due to the absence of μ_2 -Q incomplete cuboidal clusters, with these water molecules being defined according to their relative position with respect to the M' center and the plane formed by the three M centres: those that are below this plane and farther to M' are labeled as α and those the plane and closer to M' are called β . On the basis of measurements of the water exchange rates in the oxo cluster $[Mo_3O_4(H_2O)_9]^{4+}$,^{22–24} it was established that the *c* site is less labile than *d* by several orders of magnitude, and this makes the rates of substitution of both types of water very different and easy to resolve. Actually, in most substitution kinetic studies on these kinds of clusters, the data can be fitted by a single exponential, although sometimes a slower drift is observed that is often ignored in the discussion of the data.²⁷ The rate constant for this single kinetic step is interpreted as corresponding to substitution of the first *d* water molecules, which occurs at the three M centers with statistically controlled kinetics. The observation of statistical kinetics in substitution reactions of

M_3Q_4 and $M_3M'Q_4$ cluster aqua complexes is well documented by the comprehensive work of Sykes and co-workers,¹ but we have observed deviations from the statistical kinetics in some reactions of these clusters,²⁸ although these deviations appear in clusters containing other ancillary ligands and most examples are for reactions in nonaqueous solutions. However, the proximity of the k_{2f} and k_{3f} values in the present work poses some doubt in the sense that the successive measured rate constants measured could correspond to substitution of the three β water molecules (equivalent to the *c* type in M_3Q_4 clusters) with nonstatistical kinetics. Unfortunately, we have been unable to isolate and characterize the reaction product of **1** with an excess of thiocyanate, so that we cannot decide if the electronic spectrum observed at the end of the kinetic experiments corresponds to $[W_3(Pd(SCN))Se_4(NCS)_3(H_2O)_6]$ or to $[W_3(Pd(SCN))Se_4(NCS)_9]^{6-}$ species. For this reason, we decided to study the kinetics of thiocyanate substitution in a cluster for which the reaction product has been structurally characterized and its electronic spectrum is known. Although the electronic spectrum of the $[W_3Se_4(NCS)_9]^{5-}$ cluster has been reported,²⁹ the kinetics of its formation from the corresponding aqua complex has not been studied. For this reason, we selected $[W_3S_4(H_2O)_9]^{4+}$, from which $[W_3S_4(NCS)_9]^{5-}$ can be prepared, for our kinetic studies. The structure of the latter complex has been resolved³⁰ and shows three N-coordinated thiocyanate ligands at each metal center; the electronic spectrum of this complex has also been reported in both aqueous³⁰ and acetonitrile solutions.³¹

Reexamination of the Kinetics of Reaction of $[W_3S_4(H_2O)_9]^{4+}$ with SCN^- . The kinetics of reaction between $[W_3S_4(H_2O)_9]^{4+}$ and SCN^- was originally studied about 2 decades ago.²⁷ Although a single kinetic step with statistical kinetics was reported in the first work, a second kinetic step was reported later.³² However, the kinetics was monitored in both cases at single wavelength only, and the development in recent years of reliable diode-array detectors for stopped-flow machines, as well as of the programs for the global analysis of kinetic data, allows for a more detailed kinetic study by measuring and analyzing simultaneously the absorbance changes at the whole set of wavelengths within a given spectral interval. Thus, Figure 12 shows typical spectral

(27) Nasreldin, M.; Olatunji, A.; Dimmock, P. W.; Sykes, A. G. *J. Chem. Soc., Dalton Trans.* **1990**, 1765.

(28) (a) Algarra, A. S. G.; Basallote, M. G.; Fernandez-Trujillo, M. J.; Llusar, R.; Safont, V. S.; Vicent, C. *Inorg. Chem.* **2006**, *45*, 5774. (b) Algarra, A. G.; Basallote, M. G.; Feliz, M.; Fernandez-Trujillo, M. J.; Llusar, R.; Safont, V. S. *Chem.—Eur. J.* **2006**, *12*, 1413. (c) Algarra, A. G.; Basallote, M. G.; Castillo, C. E.; Corao, C.; Llusar, R.; Fernandez-Trujillo, M. J.; Vicent, C. *Dalton Trans.* **2006**, 5725. (d) Algarra, A. G.; Basallote, M. G.; Fernandez-Trujillo, M. J.; Guillamon, E.; Llusar, R.; Segarra, M. D.; Vicent, C. *Inorg. Chem.* **2007**, *46*, 7668. (29) Fedin, V. P.; Sokolov, M. N.; Virovets, A. V.; Podberzskaya, N. V.; Fedorov, V. Y. *Polyhedron* **1992**, *11*, 2973. (30) Shibahara, T.; Kohda, K.; Ohtsui, A.; Yasuda, K.; Kuroya, H. *J. Am. Chem. Soc.* **1986**, *108*, 2757. (31) Fedin, V. P.; Sokolov, M. N.; Gerasko, O. A.; Kolesov, B. A.; Fedorov, V. Y.; Mironov, A. V.; Yufit, D. S.; Slovohtov, Y. L.; Struchkov, Y. T. *Inorg. Chim. Acta* **1990**, *175*, 217. (32) Routledge, C. A.; Sykes, A. G. *J. Chem. Soc., Dalton Trans.* **1992**, 325. (33) Shibahara, T.; Sakane, G.; Maeyama, M.; Kobashi, H.; Yamamoto, T.; Watase, T. *Inorg. Chim. Acta* **1996**, *251*, 207. (34) Hernández-Molina, R.; Sokolov, M. N.; Clausen, M.; Clegg, W. *Inorg. Chem.* **2006**, *45*, 10567.

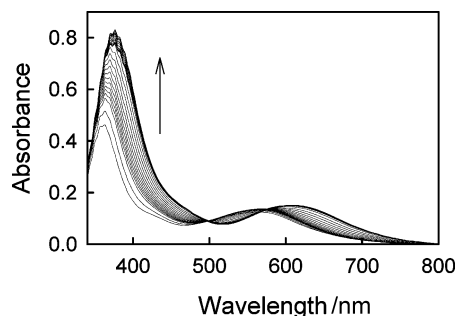


Figure 12. Typical spectral changes observed during the reaction of $[\text{W}_3\text{S}_4(\text{H}_2\text{O})_9]^{4+}$ with SCN^- in 2.0 M Hpts/Lipts. A total of 500 spectra were acquired during 1000 s with a logarithmic time base, although only some of the spectra are plotted for simplicity.

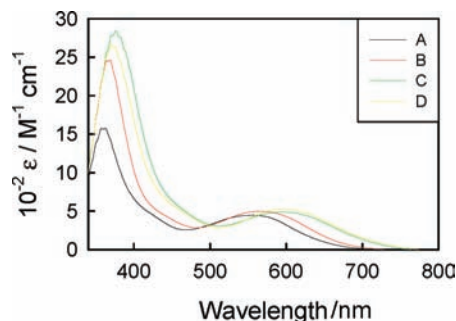


Figure 13. Spectra calculated by fitting the spectral changes in Figure 12 to a kinetic model with three consecutive exponentials. The nomenclature of the different species follows that in eq 6 but is limited to three consecutive processes.

changes for this reaction. It is important to note that the final spectra in these experiments agree within the error with those reported for $[\text{W}_3\text{S}_4(\text{NCS})_9]^{5-}$,^{30,33,34} thus showing unequivocally that the whole monitored process consists of substitution of the nine-coordinated water molecules. However, because these changes can be satisfactorily fitted by a kinetic model with three consecutive exponentials, the operation of statistical kinetics for the three resolved steps is demonstrated. The spectra calculated for the different species are included in Figure 13, and the dependence of the observed rate constants with respect to the concentration of thiocyanate is illustrated in Figure 14. Three sets of experiments were carried out in the presence of 2.0, 1.0, and 0.5 M Hpts, and in all cases, there is a linear dependence with respect to the concentration of entering ligand, although a nonzero intercept is only evident in the case of $k_{2\text{obs}}$. The values of the rate constants resulting from the data fit by eq 7 are $k_{1f} = 26 \pm 1 \text{ M}^{-1} \text{ s}^{-1}$, $k_{2f} = 4.3 \pm 0.1 \text{ M}^{-1} \text{ s}^{-1}$, $k_{2r} = (5.0 \pm 0.3) \times 10^{-2} \text{ s}^{-1}$, and $k_{3f} = 0.60 \pm 0.03 \text{ M}^{-1} \text{ s}^{-1}$ in 2.0 M Hpts; $k_{1f} = 39.1 \pm 0.7 \text{ M}^{-1} \text{ s}^{-1}$, $k_{2f} = 4.1 \pm 0.1 \text{ M}^{-1} \text{ s}^{-1}$, $k_{2r} = (4.3 \pm 0.4) \times 10^{-2} \text{ s}^{-1}$, and $k_{3f} = 0.153 \pm 0.007 \text{ M}^{-1} \text{ s}^{-1}$ in 1.0 M Hpts/1.0 M Lipts; and $k_{1f} = 75 \pm 1 \text{ M}^{-1} \text{ s}^{-1}$, $k_{2f} = 3.9 \pm 0.1 \text{ M}^{-1} \text{ s}^{-1}$, and $k_{2r} = (6.7 \pm 0.3) \times 10^{-2} \text{ s}^{-1}$ in 0.5 M Hpts/1.5 M Lipts. No resolved values of rate constants for the third step could be obtained in the latter case because the $k_{3\text{obs}}$ rate constants show erratic changes with $[\text{NCS}^-]$, probably because of the accumulation of errors.

In their previous stopped-flow kinetic study of the same reaction,²⁷ Nasreldin et al. monitored the process at 314 nm and reported data only for the first step, although small

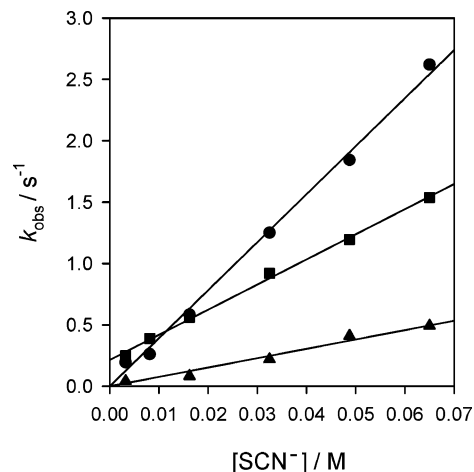
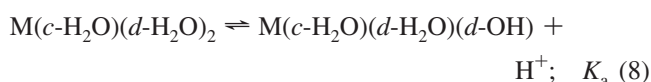
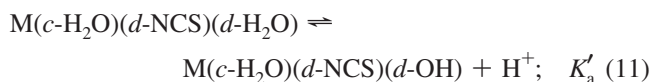
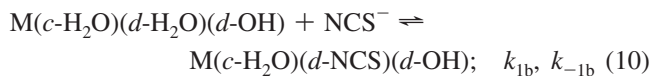
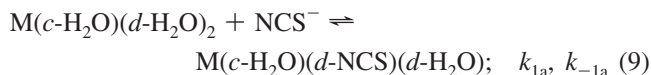


Figure 14. Plots showing the linear dependence of $k_{1\text{obs}}$ (●), $5k_{2\text{obs}}$ (■), and $50k_{3\text{obs}}$ (▲) with respect to the entering ligand concentration in the reaction of $[\text{W}_3\text{S}_4(\text{H}_2\text{O})_9]^{4+}$ with SCN^- (25.0 °C, 1.0 M Hpts/1.0 M Lipts).

contributions from a second stage were noted. Reported values of k_{1f} were $k_{1f} = 38 \pm 1 \text{ M}^{-1} \text{ s}^{-1}$ and $k_{1r} = (2.53 \pm 0.08) \times 10^{-2} \text{ s}^{-1}$ in 2.0 M HClO_4 , $k_{1f} = 59 \pm 1 \text{ M}^{-1} \text{ s}^{-1}$ and $k_{1r} = (3.54 \pm 0.07) \times 10^{-2} \text{ s}^{-1}$ in 1.0 M HClO_4 /1.0 M LiClO_4 , and $k_{1f} = 86 \pm 2 \text{ M}^{-1} \text{ s}^{-1}$ and $k_{1r} = (5.0 \pm 0.1) \times 10^{-2} \text{ s}^{-1}$ in 0.5 M HClO_4 /1.5 M LiClO_4 .²⁷ Later, the kinetics of the second, slower, process was studied by conventional spectrophotometry and the observed rate constant was found to be independent of the SCN^- concentration and assigned to an isomerization process ($k_{\text{isom}} = 1 \times 10^{-4} \text{ s}^{-1}$ in 2.0 M HClO_4).³² The magnitude of this constant is significantly smaller than any of those measured in the present work, and we have not found any evidence of an isomerization step following the three resolved steps in Figure 14. Probably, the different supporting electrolytes and the measurement of the isomerization step as a separate kinetic process without consideration of previous processes are responsible for these differences. In contrast, the agreement between the k_{1f} values obtained in both studies is quite good, with the small differences surely being caused by the separate study of the different steps in the previous works. Actually, in both cases there is a clear increase of k_{1f} when the H^+ concentration is reduced, which can be interpreted in terms of the formation of the $\text{M}-\text{OH}$ conjugate-base form, with the OH^- ligand resulting from acid dissociation from one of the d -type coordinated water molecules.²⁷ For a single metal ion, the process would occur as represented by eqs 8–11 (charges ignored for simplicity), where eq 8 represents a rapid equilibrium of the formation of the conjugate base, eqs 9 and 10 represent the reversible substitution processes in the starting complex and its conjugate base, and eq 11 takes into account the rapid equilibrium of the formation of the conjugate base in the thiocyanate-substituted complex.





The expressions derived from this mechanism for the forward and reverse rate constants are given in eqs 12 and 13.²⁴ If the reaction is considered to proceed exclusively through the conjugate-base pathway,²³ the equation can be rewritten as in eq 14, and the values derived from this analysis are $k_{1b} = (1.4 \pm 0.8) \times 10^2 \text{ M}^{-1} \text{ s}^{-1}$ and $K_a = 0.4 \pm 0.2 \text{ M}^{-1}$ for the data in the present work and $k_{1b} = (1.4 \pm 0.1) \times 10^2 \text{ M}^{-1} \text{ s}^{-1}$ and $K_a = 0.7 \pm 0.1 \text{ M}^{-1}$ for the literature²⁷ data (see Figure 15). In the previous work, the data were obtained over a wider range of $[\text{H}^+]$ and the plot showed a curvature that allowed the determination of the three components: $k_{1a} = 11.9 \pm 0.5 \text{ s}^{-1}$, $k_{1b} = 192 \pm 6 \text{ M}^{-1} \text{ s}^{-1}$, and $K_a = 0.35 \pm 0.01 \text{ M}^{-1}$ in 2.0 M $\text{HClO}_4/\text{LiClO}_4$.²⁷ In any case, the agreement between the results obtained in both studies is very good, with the differences being easily understood in terms of the differences in the experimental conditions, the analysis of the data, and the errors associated with the measurements and analysis.

$$k_{1f} = (k_{1a}[\text{H}^+] + k_{1b}K_a)/([\text{H}^+] + K_a) \quad (12)$$

$$k_{1r} = (k_{-1a}[\text{H}^+] + k_{-1b}K'_a)/([\text{H}^+] + K'_a) \quad (13)$$

$$1/k_{1f} = (1/k_{1b}) + (1/k_{1b}K_a)[\text{H}^+] \quad (14)$$

Following substitution of the first $d\text{-H}_2\text{O}$, the reaction proceeds through substitution of the second water molecule, and this is most likely the one remaining at a d coordination site. No conjugate-base pathway is observed because the other d position is already occupied by NCS^- and so the value of k_{2f} is independent of the proton concentration. $c\text{-H}_2\text{O}$

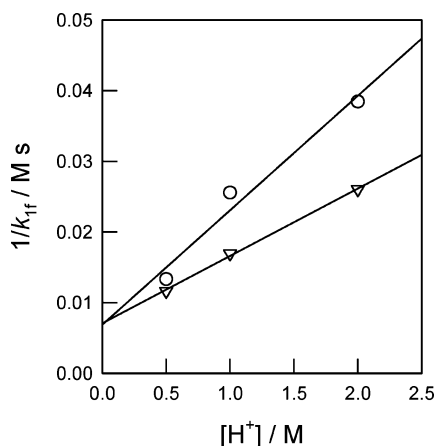


Figure 15. Plot showing the linear dependence of $1/k_{1f}$ with respect to the acid concentration for the data corresponding to the reaction of $[\text{W}_3\text{S}_4(\text{H}_2\text{O})_9]^{4+}$ with SCN^- . The triangles correspond to the data obtained in the present work and the circles to the data reported in ref 27.

does not exhibit any comparable acid dissociation. Similar comments can be made on the values of k_{2r} , although in that case, the experimental values show a somewhat larger dispersion. With regard to the k_{3f} step, the data are not so clear, although it appears that this step is inhibited as the acidity decreases, which can be qualitatively interpreted in terms of the formation of a $\text{M}(c\text{-OH})(d\text{-NCS})_2$ hydroxo complex unable to evolve into the reaction product, so that substitution can only proceed through the $\text{M}(c\text{-H}_2\text{O})(d\text{-NCS})_2$ aqua complex.

To conclude this section, it is important to note that the present reexamination of the kinetics of substitution of $[\text{W}_3\text{S}_4(\text{H}_2\text{O})_9]^{4+}$ with SCN^- confirms the operation of the statistical kinetics, so that the three metal centers in the cluster behave independently despite the extensive interaction between them (through S^{2-} bridges and metal–metal bonds). As a consequence of the statistical kinetics, substitution of each one of the water molecules coordinated at a metal center occurs at the three metal centers with rate constants that are in a 3:2:1 ratio. In addition, determination of the rate constants for the different steps reveals that the rates of substitution of the three water molecules coordinated at a given metal center are not necessarily very different, with the $k_{1f}:k_{2f}:k_{3f}$ ratio being only 43:7:1 in 2.0 M Hpts. By the combination of both ratios, it is concluded that the rate of substitution of the nine water molecules of $[\text{W}_3\text{S}_4(\text{H}_2\text{O})_9]^{4+}$ spans over a range that only slightly exceeds 2 orders of magnitude, with the ratio of the rate constants for the nine substitution processes being ca. 129:86:43:21:14:7:3:2:1. Extrapolation of these conclusions to the results obtained for cluster **1** would thus indicate that the relative rates of substitution of the nine water molecules coordinated at W centers in the Pd-containing cluster are in a 120:80:40:33:22:11:3:2:1 ratio in 2.0 M Hpts, thus showing that the relative rates for substitution of the different water molecules are not very different for both clusters.

Conclusion

The present paper reports the preparation for the first time of the W_3PdSe_4 cluster, the last one in the whole series of $\text{M}_3\text{M}'\text{Q}_4^{4+}$ cuboidal clusters ($\text{M} = \text{Mo}, \text{W}$; $\text{M}' = \text{Ni}, \text{Pd}$), whose crystal structure has been solved and shows, in the case of the aqua complex, the formation of the edge-linked double-cubane structure similar to that reported for other analogous M_3PdQ_4 clusters. The elution behavior of this compound indicates that it exists in 2.0 M Hpts solutions as the monomer **1**. The Pd center in cluster **1** is much more reactive than the W centers in the substitution reactions, as evidenced by the formation of **3**. The Pd site has been found to be effective for stabilization of the P-coordinated pyramidal form of H_3PO_2 , a process that occurs with biphasic kinetics, probably through an intermediate containing O-coordinated tetrahedral H_3PO_2 . The reactivity at the W sites has been explored in the reaction with NCS^- , which was found to occur with three resolvable kinetic steps that correspond to substitution of the three water molecules coordinated at each W center, the process occurring at the three centers with statistically controlled kinetics. The relative

rates of substitution of the nine water molecules coordinated at W centers are found to be in a 120:80:40:33:22:11:3:2:1 ratio in 2.0 M Hpts. Because the whole set of rate constants spans over a range much smaller than is usually assumed for substitution in these kinds of clusters, the kinetics of reaction of [W₃Se₄(H₂O)₉]⁴⁺ with NCS⁻ has been redetermined, using multiwavelength detection and global analysis of the kinetic data. The results obtained indicate that the nine rate constants differ by 2 orders of magnitude also in this case.

Acknowledgment. The authors thank Dr. Denis G. Samsonenko (Nikolayev Institute of Inorganic Chemistry) for his

kind help with X-ray crystallography. A.G.A. acknowledges a predoctoral grant from the Spanish Ministerio de Ciencia y Tecnología (MCT). We also thank the Spanish MCT for support through Projects BQU2005-09270 and CTQ2006-14909-C02-01.

Supporting Information Available: Electronic spectra of [W₃Se₄Pd(As(OH)₃(H₂O)₉]⁴⁺ and [W₃Se₄Pd(PhSO₂)(H₂O)₉]⁴⁺. This material is available free of charge via the Internet at <http://pubs.acs.org>.

IC802150X